

Advances and Gaps in the Knowledge of Thermodynamics and Crystallography of Acid Mine Drainage Sulfate Minerals

Juraj Majzlan*

Abstract: Acidic and metal-rich waters produced by sulfide decomposition at mining sites are termed acid mine drainage (AMD). They precipitate a number of minerals, very often sulfates. The recent advances in thermodynamic properties and crystallography of these sulfates are reviewed here. There is a reasonable amount of data for the divalent (Mg, Ni, Co, Fe²⁺, Cu, Zn) sulfates and these data may be combined with and optimized by temperature-relative humidity brackets available in the literature. For the sulfates with Fe³⁺, most data exist for jarosite; for other minerals and phases in this system, a few calorimetric studies were reported. No data whatsoever are available for the Fe²⁺-Fe³⁺ sulfates. A significant advance is the development of the Pitzer model for Fe³⁺-sulfate solutions and its confrontation with the available thermodynamic and solubility data. In summary, our knowledge about the thermodynamic properties of the AMD sulfates is unsatisfactory and fragmented.

Keywords: Acid mine drainage

Introduction

The ever-increasing demand for metals dictates the steady increase in the exploitation of ore deposits, and, to a smaller extent, attempts to recycle the useful elements. For example, 3,547 tonnes of gold were extracted in 2007.^[1] This is a large amount for a metal handled so cautiously and carefully even in the smallest quantities. Correspondingly larger amounts of other metals are needed, some of them reaching unimaginable magnitudes. The global population moves into cities which are becoming vast new ore deposits^[2] with their buildings, traffic systems, and other daily components of life. The human-induced fluxes of some elements have already exceeded the natural fluxes (e.g. Cd^[3]). Apart from creation and decomposition of the biomass, the today's human

population matches the quantities of the overall natural mass flow.^[4] The mining of ores and salts does not dominate the anthropogenic mass flow but cannot be neglected.

The extraction of ores from the lithosphere, fine grinding and disposal of unwanted waste exposes many ore minerals, in a fine particulate form, to the atmosphere and hydrosphere, thereby accelerating their decomposition rates by many orders of magnitude.^[5] The released acidity, metal cations, and anions can reach formidable levels.^[6] This phenomenon is well known under the name acid mine drainage (AMD) and is certainly not new, as can be documented by detailed descriptions in ref. [7] among others. The mineralogy of AMD systems is rich, although many minerals are only ephemeral, being washed away by rain or surface streams after a dry period. Much of the mineralogical work on AMD has been reviewed.^[5,8–10] Here I summarize the recent advances in the thermodynamics and crystallography of the sulfates found in AMD systems. The thermodynamic properties of iron oxides, halogenides, selected sulfates, and many aqueous species with iron have been critically summarized in an excellent review of Lemire *et al.*^[11] and need not to be discussed here. Because the thermodynamic properties must be referred to phases with known composition and structure, this review provides also an update for each group of considered compounds in terms of their crystal structures. This update documents how variable is this 'well known' group of structures. No comprehensive overview of the sulfate structures is necessary; this has been done

relatively recently.^[12,13] A sizeable body of data accumulated during the last ten years, partially because of interest in AMD, partially because sulfate minerals have been identified in Martian meteorites^[14] or presumed to be present on the surface of Mars (e.g. ref. [15]) and to have implications for the understanding of the ancient evolution of this planet.^[16,17]

Mineral Parageneses

Acidic, metal-rich waters can be produced by weathering of pyrite (FeS₂) or pyrrhotite (Fe_{1-x}S), rarely other sulfides, in contact with atmosphere and surface or underground water.^[5] Such weathering most commonly occurs in waste products of mining activities and the process and its products are called acid mine drainage (AMD). The composition of the two primary sulfides (pyrite and pyrrhotite) dictates the bulk ion load of the AMD waters, that is, their usually high concentration of iron, either ferrous or ferric, and sulfate. The acid waters attack and dissolve other minerals present and release their constituents into the aqueous fluids. These constituents comprise major rock-forming elements such K, Na, Mg, Ca, Al but also toxic and heavy metals and metalloids, for example Cu, Ni, Zn, Cd, As, and others. All these cations may combine with sulfate to form AMD minerals. Beside sulfates, iron oxides, be they poorly or well crystalline, are abundant. The iron oxides are powerful sorbents of many ions and thus in some cases prevent the formation of independent iron-free or iron-poor phases.

*Correspondence: Prof. Dr. J. Majzlan
Friedrich-Schiller University
Institute of Geosciences
Burgweg 11
D-07749 Jena
Tel.: +49 3641 948700
Fax: +49 3641 948602
E-mail: Juraj.Majzlan@uni-jena.de

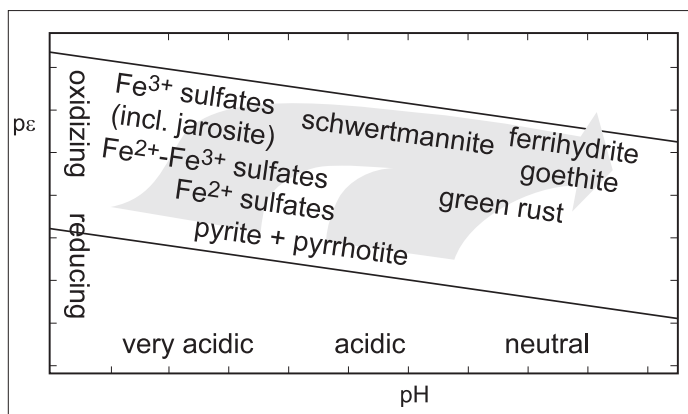


Fig. 1. Eh-pH diagram that shows two possible pathways for the evolution of an acid mine drainage system. The minerals not mentioned in the text but shown here are: goethite – α -FeOOH, green rust – Fe^{2+} - Fe^{3+} hydroxide with additional anions, schwertmannite – $\sim\text{FeO}(\text{OH})_{3/4}(\text{SO}_4)_{1/8}$, and ferrihydrite – $\sim\text{Fe}(\text{OH})_3$. Schwertmannite and ferrihydrite are poorly crystalline and metastable with respect to goethite.

In general, an AMD system proceeds through several stages of development before the final, stable or metastable but kinetically inert state is achieved.^[5] Fig. 1 shows possible evolution pathways of an AMD system. Crystallization of the soluble divalent metal sulfates depends on the availability of the divalent cations and the degree of evaporation. As the system matures, iron is being oxidized and is stored in iron sulfates or oxides, depending on the pH value of the fluids. Note that the system must achieve relatively low pH values (<2) to form the crystalline Fe^{3+} (or Fe^{2+} - Fe^{3+}) sulfates described below. It may seem, therefore, that these minerals are rare and restricted to the large AMD systems which achieve such low pH values routinely. Tosca *et al.*^[18] have shown that evaporation of pools of waters with relatively high pH (~ 3) can lead to a final pH of almost ~ 0 and precipitation of many minerals mentioned in this paper. A common example from many AMD sites are the powdery aggregates of copiapite which probably crystallize from small isolated evaporating pools of acidic waters and disappear with the first rain. As the acid-generating capacity of an AMD system vanishes, the pH rises and the final product is goethite (Fig. 1).

Divalent Metal Sulfates

Divalent metal sulfates are a diverse and large group of minerals. The divalent metals here include Fe^{2+} , Mg, Zn, Ni, Co, Mn^{2+} . The minerals progress from framework structures for the anhydrous forms to structures with isolated polyhedra or clusters thereof in heavily hydrated forms. The metals are coordinated octahedrally but because these octahedra have no tendency

to polymerize (as opposed to octahedra that house Fe^{3+}), the chemical composition of these minerals is simply $\text{MSO}_4 \cdot n\text{H}_2\text{O}$. Even with this simple composition, the variability in this group is remarkable. The structures of most of these phases have been solved earlier, reviewed in ref. [12] and further discussed in ref. [13]. A recent thorough study of the Mg sulfates identified several new phases.^[19] The structure of the MgSO_4 dihydrate (mineral sandierite^[20]), 2.5 hydrate,^[21] and the dodecahydrate (mineral meridianiite^[22]) were solved. The systems with the other divalent cations await similar attention and it is very likely that new phases exist in those systems as well.

The thermodynamic data for these phases have been summarized in an extensive compilation,^[23,24] some other data may be found in ref. [25]. The former work offers references to the older literature, the latter has, unfortunately, no references whatsoever. The reliability of the thermodynamic data varies from one mineral to the other and can be tested by constructing phase diagrams. Most data exist for the system MgSO_4 - H_2O and this system has been reviewed.^[26] The sources of data are calorimetric data (summarized in ref. [24,25], new data in ref. [26]) and the temperature-relative humidity reversals.^[27,28] They determined the stability fields of var-

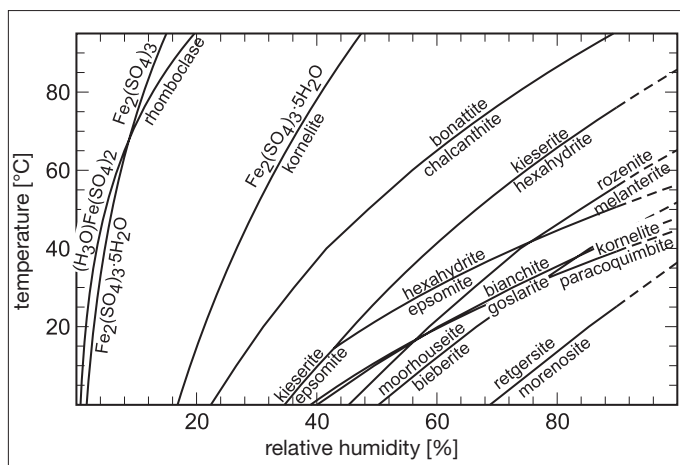


Fig. 2. Stability of sulfate minerals as a function of relative air humidity and temperature. The curves calculated from optimized thermodynamic data are: Mg sulfates,^[26] Cu, Ni, Zn, Fe^{2+} , Co sulfates (Grevel and Majzlan, in preparation). The curves for the $\text{Fe}_2(\text{SO}_4)_3 \cdot n\text{H}_2\text{O}$ were calculated from measured and estimated thermodynamic data.^[30] The curve for rhomboclase and $(\text{H}_2\text{O})\text{Fe}_2(\text{SO}_4)_2$ is the best fit to the experimental data in ref. [31]. The curves in the range of very high relative humidity are dashed because the sulfate minerals deliquesce in this region. Minerals shown in the figure: bianchite $\text{ZnSO}_4 \cdot 6\text{H}_2\text{O}$, bieberite $\text{CoSO}_4 \cdot 7\text{H}_2\text{O}$, bonattite $\text{CuSO}_4 \cdot 3\text{H}_2\text{O}$, chalcantite $\text{CuSO}_4 \cdot 5\text{H}_2\text{O}$, epsomite $\text{MgSO}_4 \cdot 7\text{H}_2\text{O}$, goslarite $\text{ZnSO}_4 \cdot 7\text{H}_2\text{O}$, hexahydrate $\text{MgSO}_4 \cdot 6\text{H}_2\text{O}$, kieserite $\text{MgSO}_4 \cdot \text{H}_2\text{O}$, kornelite $\text{Fe}_2(\text{SO}_4)_3 \cdot 7\text{H}_2\text{O}$, melanterite $\text{FeSO}_4 \cdot 7\text{H}_2\text{O}$, moorhouseite $\text{CoSO}_4 \cdot 6\text{H}_2\text{O}$, morenosite $\text{NiSO}_4 \cdot 7\text{H}_2\text{O}$, paracoquimbite $\text{Fe}_3(\text{SO}_4)_9 \cdot 9\text{H}_2\text{O}$, retgersite $\text{NiSO}_4 \cdot 6\text{H}_2\text{O}$, rhomboclase $(\text{H}_2\text{O})\text{Fe}_2(\text{SO}_4)_2 \cdot 2\text{H}_2\text{O}$, rozenite $\text{FeSO}_4 \cdot 4\text{H}_2\text{O}$.

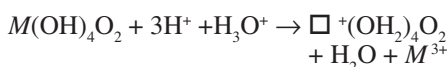
ious $\text{MgSO}_4 \cdot n\text{H}_2\text{O}$ phases by varying relative humidity and temperature. Because they were able to reverse the reactions, that is, to observe hydration of the lower hydrate and dehydration of the corresponding higher hydrate, these experiments are brackets in the sense of the brackets commonly determined for high-temperature and high-pressure silicate equilibria. The univariant curves calculated from available thermodynamic values^[24,25] significantly deviate from the experimentally observed reversals.^[27,28] To alleviate this problem, Grevel and Majzlan^[26] applied the mathematic programming analysis (*cf.* ref. [29]), a method that varies the available thermodynamic values within their uncertainties. The result of the calculations is a phase diagram constructed from optimized thermodynamic data and satisfying the experimental observations (Fig. 2). We are currently in process of optimizing the scarcer data for the Fe^{2+} , Co, Ni, and Zn sulfate phases and some preliminary results are also depicted in Fig. 2.

The mixing properties in the continuous solid solutions between Ni, Mg, and Zn sulfates heptahydrates were investigated in a series of studies.^[32–35] They showed that the thermodynamics of mixing in these solid solutions is not ideal although the Gibbs free energies of mixing are rather small, up to 0.2 kJ/mol.

Jarosite

The solid solution between jarosite s.s., natrojarosite, and hydronium jarosite is probably the most common crystalline sulfate in acid mine drainage. Jarosite is isostructural with alunite whose structure was solved by Hendricks.^[36] Recently, Sato *et al.*^[37] refined the structure of a suite of jarosite-group minerals. The numerous substitutions within jarosite can place constraints on the composition of natural fluids which precipitated this mineral.^[38,39] The structure is built by sheets of octahedra which house Fe³⁺. The sheets are decorated by sulfate tetrahedra and the monovalent ions reside between the sheets in a large site with coordination number of 12. These principal features are maintained throughout the jarosite family of minerals; deviations from the trigonal symmetry or localization of cations at otherwise vacant sites have been reported.^[40–42] The structure is further complicated by the abundance of defects and species that are difficult to detect by diffraction techniques or most types of spectroscopy.

The elusive hydronium ion is usually called upon when the monovalent cations (mostly Na and K in nature) do not occupy the 12-fold coordinated site completely. The existence of the hydronium ion in the jarosite structure is difficult to prove by diffraction techniques. Nielsen *et al.*^[43] have applied nuclear magnetic resonance spectroscopy (NMR) on the ²H nuclei in a set of synthetic, deuterated jarosite samples. They detected three different local deuterium environments, Fe₂OD, FeOD₂, and D₂O/D₃O⁺ in jarosite (Fig. 3). The paramagnetic nature of the jarosite at room temperature was helpful, and not obstructive, as it separated the signal into three easily resolvable Fermi contact shifts of $\delta \approx 237$, 70, and 0 ppm, respectively. The Fe₂OD groups are rigid in terms of the motion visible in the NMR spectra. The FeOD₂ groups, on the other hand, undergo rapid flips on the NMR time scale. They arise from the charge compensation of the Fe³⁺ vacancies and were used in these experiments to determine the concentration of the vacancies. The sites usually assumed to be occupied by monovalent cations are populated by D₂O or D₃O⁺ groups. The mechanism of vacancy introduction can be described by an exchange reaction



where *M* is either Al³⁺^[44] or Fe³⁺. Therefore, the hydronium ions are consumed by the vacancies and can only exist in the near-stoichiometric regions in jarosite (or alunite, the Al analogue of jarosite). This conclusion was confirmed by the study of a series of stoichiometric and non-stoichio-

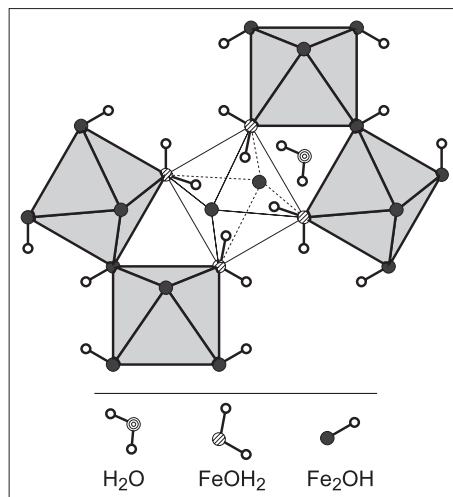


Fig. 3. A segment from the structure of jarosite showing a vacancy at the Fe³⁺ site. Note that the H₂O molecule shown is located approximately (1/6)c above the plane defined by the Fe³⁺ cations.

metric samples by NMR.^[43,44] The entire picture is further complicated by the fact that the A site may not be fully occupied. The occupancy of this site was only 91% in pure synthetic jarosite,^[45] showing that the common assumption that the difference between 100% and (Na+K) content on the A site is the hydronium ion may be in error. Gale *et al.*^[46] used atomistic simulation of a hydronium alunite structure and found that the H₃O⁺ ion assumes 12 symmetry-related positions in its cavity. In none of these positions, however, coincides the penetrative three-fold symmetry axis with the local three-fold axis of the H₃O⁺ ion.

There was a significant effort expended to synthesize stoichiometric, defect-free jarosite samples. One synthesis route uses metallic iron as a starting product and the consequent slow supply of Fe³⁺ into the solution as the means for the assembly of a stoichiometric structure.^[47] This procedure also allows syntheses of jarosite phases with V³⁺ and Cr³⁺,^[48] unknown from nature, and was driven mostly by the interest in the unusual magnetic properties of jarosite.^[49] The other route is based on lowering the activity of H₂O and H₃O⁺ in the aqueous solution by massive addition of Li⁺ which does not enter the jarosite structure.^[50,51]

The earlier studies on thermodynamic properties of jarosite minerals have been summarized.^[10] They were mostly based on evaluation of the solubility of jarosite in aqueous media.^[52–56] The results of those studies where jarosite was allowed to dissolve in water (as opposed to crystallizing jarosite from a solution) could be questioned because the dissolution of jarosite could be incongruent.^[57] Stoffregen^[58] adopted a different approach, that is, evaluation of high-temperature equilibria between jarosite and its decomposition

products. The thermodynamic properties of jarosite were then derived by extrapolation of the data to 298.15 K, using the activity-molality relation of the aqueous ions valid only for *T* = 298.15 K. In addition, Stoffregen^[58] reported that jarosite decomposes either to hematite or Fe(OH)SO₄, depending on the activity of sulfate in the aqueous solution. We have found (Majzlan, unpublished) that jarosite decomposes invariably to a mixture of hematite and yavapaiite (KFe(SO₄)₂) at 0.2 GPa and temperatures of 200–600 °C. To compound the problem further, in most of the studies cited in this paragraph, jarosite was implicitly assumed to be stoichiometric, although, as discussed above, the preparation of a stoichiometric phase requires significant effort.

An alternative approach is to measure the formation enthalpy and standard entropy of these phases separately and to combine them into ΔG_f° values. Drouet and Navrotsky^[59] measured the formation enthalpy of a series of jarosite phases by high-temperature calorimetry and proposed the best thermodynamic values. Their best values, however, do not satisfy the relationship $\Delta G_f^\circ = \Delta H_f^\circ - T\Delta S_f^\circ$, and therefore should be used with caution, if at all. They also measured the formation enthalpy of hydronium jarosite, later re-measured (using the same sample) by acid-solution calorimetry.^[45] The discrepancy between the two ΔH_f° values is astounding, almost 30 kJ/mol. The reason for such large discrepancy is not clear, but the data (measured enthalpy and entropy) in ref. [45] show internal consistency with the available phase diagrams and are therefore considered to be superior. The formation enthalpy of Pb-jarosite was recently reported.^[60]

The only so far published low-temperature heat capacity and entropy data are those for hydronium jarosite.^[45] Majzlan *et al.*^[61] measured *C_p* and *S*^o for a series of stoichiometric jarosite phases and a non-stoichiometric potassium-rich jarosite. Striking is the difference in the estimate of *S*^o for the K-jarosite of 388.9 J·mol⁻¹·K⁻¹^[58] and the experimental value of 427.4 J·mol⁻¹·K⁻¹.^[61]

Such differences further underscore the need for experimental measurements, especially in systems where vacancies, defects, deviations from nominal stoichiometry, and unusual magnetic properties are the rule, not an exception.

Fe(III) Sulfates except Jarosite

These minerals are chemically and structurally variable (see Table 1 for a list with the chemical formulae). In general, the structures progressively depolymerize with the increasing hydration state, passing from the anhydrous framework structures

Table 1. Sulfates of Fe³⁺ which may be found in the AMD systems

AFe ₃ (SO ₄) ₂ (OH) ₆	jarosite group (A = Na ⁺ , K ⁺ , H ₃ O ⁺)
AFe ₃ (SO ₄) ₆ (OH) ₂ ·20H ₂ O	copiapite group (A = 2/3Fe ³⁺ , 2/3Al ³⁺ , Mg, Zn, Fe ²⁺)
Fe(OH)SO ₄ ·nH ₂ O	butlerite, parabutlerite, fibroferrite
(Fe,Al) ₂ (SO ₄) ₃ ·nH ₂ O	mikasaite, lausenite, kornelite, coquimbite, paracoquimbite, quenstedtite
Fe ₂ O(SO ₄) ₂ ·nH ₂ O	hohmannite, metahohmannite, amarantite
(H ₃ O) ₂ Fe(SO ₄) ₂ ·2H ₂ O	rhombochase
KFe(SO ₄) ₂ ·nH ₂ O	yavapaiite, krausite, goldichite
Na ₂ Fe(OH)(SO ₄) ₂ ·3H ₂ O	sideronatrite
Na ₃ Fe(SO ₄) ₃ ·3H ₂ O	ferrinatrite
MgFe(SO ₄) ₂ (OH)·7H ₂ O	botryogen
NaMg ₂ Fe ₅ (SO ₄) ₇ (OH) ₆ ·33H ₂ O	slavikite

to heavily hydrated structures with isolated polyhedra or polyhedral clusters.

In their thorough study, Posnjak and Merwin^[62] identified a number of phases whose structure is today known. The last remaining structures were those of Fe₂(SO₄)₃·5H₂O,^[63] and (H₃O)Fe(SO₄)₂.^[64] The former phase may or may not correspond to the mineral lausenite and the question can be probably solved only if this rare mineral is found again.^[63] The structure of metahohmannite was solved from powder XRD data,^[65] a remarkable work given the triclinic symmetry and the presence of impurities in the sample. It may seem from the previous few sentences that little remains to be done with the crystal structures of Fe(III) sulfates. This impression is, of course, false. Interesting and unusual variations were found among the phases close to coquimbite;^[66] with an increasing Al content, the coquimbite structure changes from having isolated polyhedral clusters

to infinite chains. At least two slightly different structures can be recognized among the copiapite-group minerals.^[67] Voltaite, a phase with cubic morphology but anisotropic behavior in crossed nicols, was shown to have a slight tetragonal distortion.^[68] In their study of hydration and dehydration of the Fe(III) sulfates, Xu *et al.*^[69] detected an unknown phase or phases. Obviously, these minerals still hide many secrets which await to be discovered.

Much less is known about the thermodynamics of these phases. Hemingway *et al.*^[70] estimated the properties of a number of these phases. Although it could be argued that the absence of data at that time justified the estimates, the phase relationships in systems with a delicate thermodynamic balance cannot be constructed only with estimates. The Fe(III) sulfates are such a system.

Several papers addressed the thermodynamics of anhydrous Fe₂(SO₄)₃; its

trigonal polymorph is the mineral mikasaite, the monoclinic polymorph is so far unknown from nature. The formation enthalpy was measured or estimated in refs [71–73] and the values roughly agree. The entropy values^[73,74] on the other hand, disagree significantly, mostly because Pankratov and Weller^[74] measured data down to 50 K and then extrapolated to 0 K. Doing so, they missed most of the magnetic entropy and underestimated the total entropy at T = 298.15 K by about 10%. This problem was avoided by measuring heat capacity down to 1 K, well below the magnetic transition.^[73]

Enthalpies of formation were measured by acid-solution calorimetry for Fe₂(SO₄)₃·5H₂O, kornelite, coquimbite, paracoquimbite, rhombochase, and ferricopiapite.^[30,75] Entropy estimates were presented for all these phases in the two publications. Ackermann *et al.*^[30] have shown that, using reasonable estimates of entropies, a sensible phase diagram for the Fe₂(SO₄)₃·nH₂O phases can be constructed (Fig. 2). Such phase diagram can be further combined and optimized with the temperature-relative humidity brackets,^[69,76,77] although these experiments may be plagued by sluggishness, disequilibrium, and the presence of unknown phases. These brackets are now not only available for the Fe₂(SO₄)₃·nH₂O phases (i.c.) but also for the pair (H₃O)Fe(SO₄)₂-rhombochase^[31] (Fig. 2). An approximate Eh-pH phase diagram (Fig. 4) agrees with the field observations but a diagram that shows the coexistence of the aqueous phase with the individual minerals^[62,80] deviates, at least visually, much from the experimental data (Fig. 5). The discrepancy in the magnitude

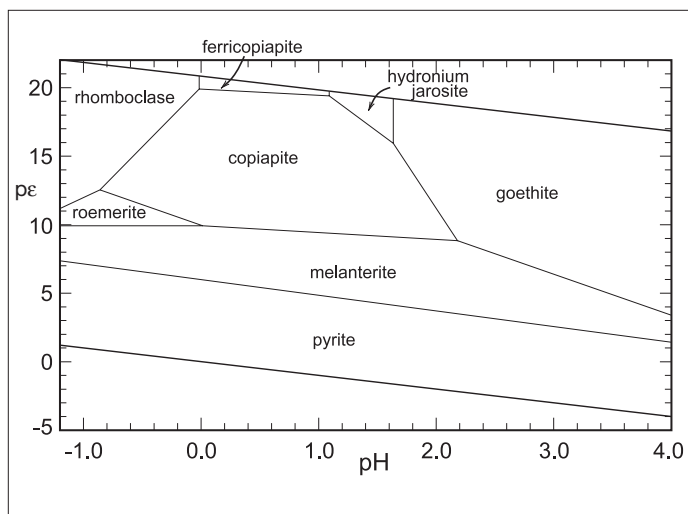


Fig. 4. A schematic pH-Eh diagram for pyrite, melanterite, and a suite of Fe³⁺ sulfate and oxide minerals. The fixed activities of aqueous species are: $a(\text{SO}_4^{2-}) = 3.50$, $a(\text{Fe}^{3+}) = a(\text{Fe}^{2+}) = 1.20$, $a(\text{H}_2\text{O}) = 0.75$. Data for pyrite from ref. [78]. Data for melanterite from optimized thermodynamic data (Grevil and Majzlan, in preparation). Data for the Fe³⁺ phases: hydronium jarosite,^[45] rhombochase and ferricopiapite,^[75] goethite,^[79] copiapite and roemerite – adjusted estimates from ref. [70].

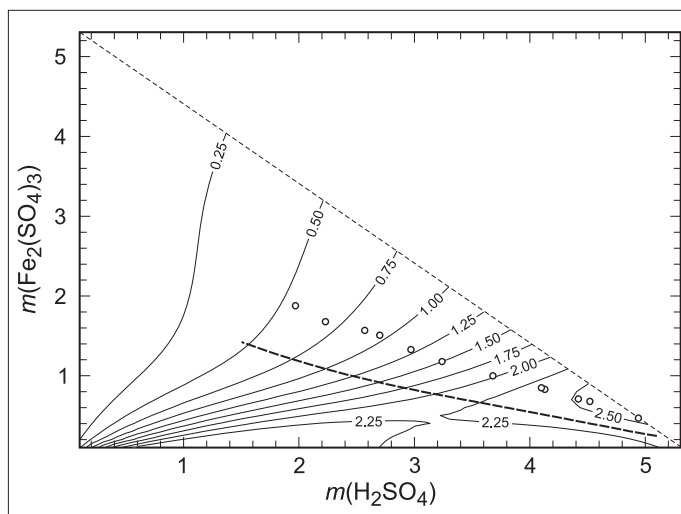


Fig. 5. Contours of the ratio of molalities of HSO₄⁻ and SO₄²⁻ as predicted by the Pitzer model parameters from ref. [81]. The thick dashed line represents the composition of the solution in equilibrium with rhombochase, (H₃O)₂Fe(SO₄)₂·2H₂O, calculated from the Pitzer model^[81] and thermodynamic data from ref. [75]. The circles show the experimentally determined solution compositions in equilibrium with rhombochase from refs [82–84].

of the thermodynamic values is, however, not very large, because the position of the curve plotted in Fig. 5 is a very sensitive function of the thermodynamic data. Tosca *et al.*^[81] concluded that the extent of the divergence is 'encouraging' and I would only add that it is a good starting point for further studies. Thermodynamic data for all other minerals listed in Table 1 but not explicitly mentioned in this paragraph are unknown. Thermodynamic properties of Fe²⁺-Fe³⁺ sulfates are also unknown.

Aqueous Solutions

The thermodynamic description of the AMD systems remains incomplete if the properties of the aqueous media are unknown. The aqueous solutions typical for these systems are usually concentrated, with the extremes up to eight molal H₂SO₄ concentrations.^[6] Simple molality-activity (*e.g.* Debye-Hückel) models are not valid for such solutions. Instead, the more complicated model developed by K. Pitzer and coworkers^[85,86] can be used.

Initially, the H₂SO₄ solutions were treated with the assumption of complete dissociation.^[87] The inclusion of HSO₄⁻ provided much more reliable predictions of the properties.^[88] Lassin *et al.*^[89] have shown that at high H₂SO₄ molalities, the Pitzer model must also include H₂SO₄⁰ as a species. Pitzer model parameters have been derived for solutions containing Mg-SO₄, Fe(II)-SO₄, Ni-SO₄, Al-SO₄, and other systems (see ref. [90] for a review) relevant for the AMD waters. Proskurina *et al.*^[33] reported Pitzer coefficients for the MgSO₄-, NiSO₄-, and ZnSO₄-H₂O systems. Pitzer-model coefficients for solutions with Fe(III) and SO₄ were reported only recently by Tosca *et al.*^[81] who derived them from the isopiestic data.^[91,92] As an example, Fig. 5 depicts the speciation of SO₄²⁻ and HSO₄⁻ in the Fe(III)-sulfate solutions. The fraction of HSO₄⁻ steeply increases from infinite dilution as the H₂SO₄ molality is increased but reaches a broad minimum between 3.5–4.5 m H₂SO₄; a similar trend is seen for pure H₂SO₄ solutions.^[88] Generally, the fraction of HSO₄⁻ decreases as Fe₂(SO₄)₃ is added to the solution. An exception in this trend are solutions with high H₂SO₄ molality where the addition of Fe₂(SO₄)₃ causes an increase in the HSO₄⁻ concentration. The effect of these changes upon the structures of co-existing minerals will have to be examined in further detail. The predicted pH values vary between 2 and -2 for the molalities considered by the model in ref. [81]. It is interesting to note that solutions with very high Fe₂(SO₄)₃ molality but low H₂SO₄ molality have relatively 'high' pH values around 2. The Pitzer parameters presented^[81] describe the thermodynamic

properties of aqueous species in a wide range of H₂SO₄ and Fe₂(SO₄)₃ molalities. Care must be taken, however, for solutions where the Fe₂(SO₄)₃ molality is high and that of H₂SO₄ is low. In this case, ion pairing of Fe³⁺ and sulfate may render even this complicated model inaccurate.

Outlook and Implications

As shown in this short review, the thermodynamic database for the AMD sulfates has expanded in the last decade so that at least preliminary phase diagrams can be drawn. Although the progress with the Fe³⁺ sulfates is 'encouraging',^[81] it is far from satisfactory. Data for the Fe²⁺-Fe³⁺ sulfates are missing and the data for the divalent sulfates, much more abundant, are in a need of critical evaluation and optimization.

The last point that needs discussion are the implications that the phase diagrams have for the prediction of the natural assemblages. First, the AMD systems abound with metastability and sluggishness. Therefore, the thermodynamic calculations only whisper about the way the system may go. Second, even if equilibrium is assumed and thermodynamic data are on hand, phase diagrams with no meaning whatsoever can be calculated because of an improper choice of phases. For example, one could choose anhydrous FeSO₄ for the diagram in Fig. 4 and argue that such phase should be found in nature. It is unlikely that we will see such a diagram. Yet, there are analogous diagrams, for example, for systems (AMD or not) polluted with antimony (see ref. [93] for more information) that provide a misleading picture about the solid and aqueous speciation of elements. Therefore, phases for construction of the phase diagrams should be always chosen carefully and critically, even if their thermodynamic data are sound.

Acknowledgements

I thank T. Armbruster for the invitation to write this review article, R. C. Peterson and J. J. Papike for the reviews, and K.-D. Grevel for the unpublished data for the divalent metal sulfates. The financial support of the *Deutsche Forschungsgemeinschaft* in projects on mineralogy, crystallography, and thermodynamics of the sulfate minerals is greatly appreciated.

Received: April 24, 2010

- [1] 'Gold Demand Trends', Full year and fourth quarter 2007, issued by The World Gold Council and GFMS Ltd.
- [2] S. Norra, *Environ. Sci. Pollut. Res.* **2009**, *16*, 539.
- [3] P. Baccini, P. H. Brunner, 'Metabolism of the anthroposphere' Springer, Berlin, 1991.
- [4] K. Heinloth, 'Die Energiefrage – Bedarf und

- Potentiale, Nutzung, Risiken und Kosten', Vieweg, 1997.
- [5] J. L. Jambor, in 'Environmental aspects of mine wastes', Eds J. L. Jambor, D. W. Blowes, A. I. M. Ritchie, Mineralogical Association of Canada **2003**, *31*, 117.
- [6] D. K. Nordstrom, C. N. Alpers, *Proc. Natl. Acad. Sci. USA* **1999**, *96*, 3455.
- [7] A. Breithaupt, *Berg- und hüttenmännische Zeitung* **1852**, *11*, 65; J. D. Dana, 'Manual of Mineralogy' Durrie & Peck, New Haven, **1848**; H. Rose, *Ann. Phys.* **1833**, *27*, 309.
- [8] J. L. Jambor, D. K. Nordstrom, C. N. Alpers, *Rev. Mineral. Geochem.* **2000**, *40*, 303.
- [9] J. M. Bigham, D. K. Nordstrom, *Rev. Mineral. Geochem.* **2000**, *40*, 351.
- [10] R. E. Stoffregen, C. N. Alpers, J. L. Jambor, *Rev. Mineral. Geochem.* **2000**, *40*, 454.
- [11] R. J. Lemire, U. Berner, C. Musikas, D. A. Palmer, P. Taylor, O. Tochiyama, 'Chemical thermodynamics of iron', Nuclear Energy Agency (Organisation for Economic Cooperation and Development), **2010**.
- [12] F. C. Hawthorne, S. V. Krivovichev, P. C. Burns, *Rev. Mineral. Geochem.* **2000**, *40*, 1.
- [13] M. Schindler, D. M. C. Humnicki, F. C. Hawthorne, *Can. Mineral.* **2006**, *44*, 1403.
- [14] F. M. McCubbin, N. J. Tosca, A. Smirnov, H. Nekvasil, A. Steele, M. Fries, D. H. Lindsley, *Geochim. Cosmochim. Acta* **2009**, *73*, 4907.
- [15] S. W. Squyres, J. P. Grotzinger, R. E. Arvidson, J. F. Bell, W. Calvin, P. R. Christensen, B. C. Clark, J. A. Crisp, W. H. Farrand, K. E. Herkenhoff, J. R. Johnson, G. Klingelhöfer, A. H. Knoll, S. M. McLennan, H. Y. McSween, R. V. Morris, J. W. Rice, R. Rieder, L. A. Soderblom, *Science* **2004**, *306*, 1709.
- [16] J. J. Papike, J. M. Karner, C. K. Shearer, *Geochim. Cosmochim. Acta* **2006**, *70*, 1309.
- [17] J. J. Papike, P. V. Burger, J. M. Karner, C. K. Shearer, V. W. Lueth, *Am. Mineral.* **2007**, *92*, 444.
- [18] N. J. Tosca, S. M. McLennan, B. C. Clark, J. P. Grotzinger, J. A. Hurowitz, A. H. Knoll, C. Schröder, S. W. Squyres, *Earth Planet. Sc. Lett.* **2005**, *240*, 122.
- [19] S. J. Chipera, D. T. Vaniman, *Geochim. Cosmochim. Acta* **2007**, *71*, 241.
- [20] H. W. Ma, D. L. Bish, H. W. Wang, S. J. Chipera, *Am. Mineral.* **2009**, *94*, 622.
- [21] H. W. Ma, D. L. Bish, H. W. Wang, S. J. Chipera, *Am. Mineral.* **2009**, *94*, 1071.
- [22] R. C. Peterson, R. Wang, *Geology* **2006**, *34*, 957.
- [23] C. W. DeKock, *U.S. Bur. Mines, Inf. Circ.* **1982**, 8910.
- [24] C. W. DeKock, *U.S. Bur. Mines, Inf. Circ.* **1986**, 9081.
- [25] D. D. Wagman, W. H. Evans, V. B. Parker, R. H. Schumm, I. Halow, S. M. Bailey, K. L. Churney, R. L. Nuttall, *J. Phys. Chem. Ref. Data* **1982**, *11*, Suppl. 2.
- [26] K.-D. Grevel, J. Majzlan, *Geochim. Cosmochim. Acta* **2009**, *73*, 6805.
- [27] I.-M. Chou, R. R. Seal, *Astrobiology* **2003**, *3*, 619.
- [28] I.-M. Chou, R. R. Seal, *J. Geophys. Res. – Planets* **2007**, *112*, 10.1029/2007JE002898.
- [29] R. G. Berman, M. Engi, H. J. Greenwood, T. H. Brown, *J. Petrol.* **1986**, *27*, 1331.
- [30] S. Ackermann, T. Armbruster, B. Lazic, S. Doyle, K.-D. Grevel, J. Majzlan, *Am. Mineral.* **2009**, *94*, 1620.
- [31] W. Xu, J. Parise, J. Hanson, *Am. Mineral.* (submitted) **2010**.
- [32] I. A. Kasatkin, E. B. Treivus, T. I. Ivanova, *Russ. J. Phys. Ch.* **2000**, *73*, 1880.
- [33] O. V. Proskurina, E. S. Mal'tseva, A. V. Rummyantsev, L. V. Puchkov, *Russ. J. Phys. Ch.* **2001**, *75*, 343.
- [34] O. V. Proskurina, L. V. Puchkov, A. V. Rummyantsev, *Russ. J. Phys. Ch.* **2001**, *75*, 163.
- [35] O. V. Proskurina, A. V. Rummyantsev, N. A.

- Charykov, *Russ. J. Phys. Ch.* **2002**, 76, 1399.
- [36] S. B. Hendricks, *Am. Mineral.* **1937**, 22, 773.
- [37] E. Sato, I. Nakai, R. Miyawaki, S. Matsubara, *Neues Jb. Miner. Abh.* **2009**, 185, 313.
- [38] G. A. Desborough, K. S. Smith, H. A. Lowers, G. A. Swayze, J. M. Hammarstrom, S. F. Diehl, R. W. Leinz, R. L. Driscoll, *Geochim. Cosmochim. Acta* **2010**, 74, 1041.
- [39] P. V. Burger, J. J. Papike, C. K. Shearer, J. M. Karner, *Geochim. Cosmochim. Acta* **2009**, 73, 3248.
- [40] J. Göttlicher, B. Gasharova, H. Bernotat-Wulff, *Abstr. Programs-Geol. Sci. Am.* **2000**, 32, A180.
- [41] I. E. Grey, W. G. Mumme, P. Bordet, S. J. Mills, *Can. Mineral.* **2008**, 46, 1355.
- [42] I. E. Grey, W. G. Mumme, S. J. Mills, W. D. Birch, N. C. Wilson, *Am. Mineral.* **2009**, 94, 676.
- [43] U. G. Nielsen, J. Majzlan, C. P. Grey, *Chem. Mater.* **2008**, 20, 2234.
- [44] U. G. Nielsen, J. Majzlan, B. Phillips, M. Ziliox, C. P. Grey, *Am. Mineral.* **2007**, 92, 587.
- [45] J. Majzlan, R. Stevens, J. Boerio-Goates, B. F. Woodfield, A. Navrotsky, M. Crawford, P. Burns, T. G. Amos, *Phys. Chem. Miner.* **2004**, 31, 518.
- [46] J. D. Gale, K. Wright, K. A. Hudson-Edwards, *Am. Mineral.* **2010**, 95, 1109.
- [47] D. Grohol, D. G. Nocera, D. Papoutsakis, *Phys. Rev. B* **2003**, 67, 064401.
- [48] D. Grohol, D. G. Nocera, *J. Am. Chem. Soc.* **2002**, 124, 2640.
- [49] D. Grohol, D. G. Nocera, *Chem. Mater.* **2007**, 19, 3061.
- [50] L. C. Basciano, R. C. Peterson, *Am. Mineral.* **2007**, 92, 1464.
- [51] L. C. Basciano, R. C. Peterson, *Am. Mineral.* **2008**, 93, 853.
- [52] A. V. Zotov, G. D. Mironova, V. L. Rusinov, *Geokhimiya* **1973**, 5, 739.
- [53] C. H. M. Kashkay, Y. U. B. Borovskaya, M. A. Babazad, *Geochem. Int.* **1975**, 12, 115.
- [54] C. N. Alpers, D. K. Nordstrom, J. W. Ball, *Sci. Geol. Bull.* **1989**, 4, 281.
- [55] D. Baron, D. Palmer, *Geochim. Cosmochim. Acta* **1996**, 60, 185.
- [56] D. Baron, D. Palmer, *Geochim. Cosmochim. Acta* **2002**, 66, 2841.
- [57] A. M. L. Smith, K. A. Hudson-Edwards, W. E. Dubbin, K. Wright, *Geochim. Cosmochim. Acta* **2006**, 70, 608.
- [58] R. E. Stoffregen, *Geochim. Cosmochim. Acta* **1993**, 57, 2417.
- [59] C. Drouet, A. Navrotsky, *Geochim. Cosmochim. Acta* **2003**, 67, 2063.
- [60] F. L. Forray, A. M. L. Smith, C. Drouet, A. Navrotsky, K. Wright, K. A. Hudson-Edwards, W. E. Dubbin, *Geochim. Cosmochim. Acta* **2010**, 74, 215.
- [61] J. Majzlan, P. Glasnák, R. A. Fisher, M.-A. White, M. Johnson, B. Woodfield, J. Boerio-Goates, *Phys. Chem. Miner.* **2010**, 37, 635.
- [62] E. Posnjak, H. E. Merwin, *J. Am. Chem. Soc.* **1992**, 44, 1965.
- [63] J. Majzlan, C. Botez, P. W. Stephens, *Am. Mineral.* **2005**, 90, 411.
- [64] R. C. Peterson, E. Valyashko, R. Want, *Can. Mineral.* **2009**, 47, 625.
- [65] F. Scordari, G. Ventruti, A.F. Gualtieri, *Am. Mineral.* **2004**, 89, 365.
- [66] F. Demartin, C. Castellano, C. Gramaccioli, I. Camprostrini, *Can. Mineral.* **2010**, 48, 323.
- [67] J. Majzlan, R. Michallik, *Mineral. Mag.* **2007**, 71, 557.
- [68] A. Ertl, M. D. Dyar, J. M. Hughes, F. Brandstatter, M. E. Gunter, M. Prem, R. C. Peterson, *Can. Mineral.* **2008**, 46, 661.
- [69] W. Xu, N. J. Tosca, S. M. McLennan, J. B. Parise, *Am. Mineral.* **2009**, 94, 1629.
- [70] B. S. Hemingway, R. R. Seal, I. M. Chou, *U.S. Geol. Survey, Open File Report* **2002**, 02-161.
- [71] R. Barany, L. H. Adami, *U.S. Bur. Mines, Rep. Invest.* **1965**, 6687.
- [72] H. H. Kellogg, *T. Metall. Soc. AIME* **1964**, 230, 1622.
- [73] J. Majzlan, A. Navrotsky, R. Stevens, M. Donaldson, B. F. Woodfield, J. Boerio-Goates, *J. Chem. Thermodyn.* **2005**, 37, 802.
- [74] L. B. Pankratz, W. W. Weller, *U.S. Bur. Mines, Rep. Invest.* **1969**, 7280.
- [75] J. Majzlan, A. Navrotsky, B. McCleskey, C. N. Alpers, *Eur. J. Mineral.* **2006**, 18, 175.
- [76] E. A. Hasenmueller, D. L. Bish, *Lunar Planet. Sci. Conf.* **2005**, #1164.
- [77] S. J. Chipera, D. T. Vaniman, D. L. Bish, *Lunar Planet. Sci. Conf.* **2007**, #1409.
- [78] R. A. Robie, B. S. Hemingway, 'Thermodynamic properties of minerals and related substances at 298.15 K and 1 bar (10⁵ Pascals) and at higher temperatures', *U.S. Geol. Survey Bull.* **1995**, 2131.
- [79] J. Majzlan, K.-D. Grevel, A. Navrotsky, *Am. Mineral.* **2003**, 88, 855.
- [80] H. E. Merwin, E. Posnjak, *Am. Mineral.* **1937**, 22, 567.
- [81] N. J. Tosca, A. Smirnov, S. M. McLennan, *Geochim. Cosmochim. Acta* **2007**, 71, 2680.
- [82] F. K. Cameron, C. Robinson, *J. Phys. Chem.* **1907**, 11, 641.
- [83] F. Wirth, B. Bakke, *Z. anorg. Chem.* **1914**, 87, 13.
- [84] W. H. Baskerville, F. K. Cameron, *J. Phys. Chem.* **1935**, 39, 769.
- [85] K. S. Pitzer, *J. Phys. Chem.* **1973**, 77, 2300.
- [86] K. S. Pitzer, 'Activity coefficients in electrolyte solutions', CRC Press Boca Raton **1991**.
- [87] K. S. Pitzer, R. N. Roy, L. F. Silvester, *J. Am. Chem. Soc.* **1977**, 99, 4930.
- [88] S. L. Clegg, J. A. Rard, K. S. Pitzer, *J. Chem. Soc. Faraday T.* **1994**, 90, 1875.
- [89] A. Lassin, C. Kervévan, L. André, M. Azaroual, *Goldschmidt conf.* **2009**, A724.
- [90] C. Ptacek, D. Blowes, *Rev. Mineral. Geochem.* **2000**, 40, 513.
- [91] A. V. Rummyantsev, S. Hagemann, H. C. Moog, *Z. phys. Chem.* **2004**, 218, 1089.
- [92] M. Velazquez-Rivera, D. A. Palmer, R. M. Kettler, *J. Solution Chem.* **2006**, 35, 1699.
- [93] M. Filella, P. A. Williams, N. Belzile, *Environ. Chem.* **2009**, 6, 95.